Comput Mech (2013) 51:495–503
DOI 10.1007/s00466-012-0777-8

ORIGINAL PAPER

Numerics of boundary-domain integral and integro-differential equations for BVP with variable coefficient in 3D

Richards Grzhibovskis · Sergey Mikhailov · Sergej Rjasanow

Received: 28 February 2012 / Accepted: 7 August 2012 / Published online: 25 August 2012

Abstract A numerical implementation of the direct boundary-domain integral and integro-differential equations, BDIDEs, for treatment of the Dirichlet problem for a scalar elliptic PDE with variable coefficient in a three-dimensional domain is discussed. The mesh-based discretisation of the BDIEs with tetrahedron domain elements in conjunction with collocation method leads to a system of linear algebraic equations (discretised BDIE). The involved fully populated matrices are approximated by means of the H-Matrix/adaptive cross approximation technique. Convergence of the method is investigated.

Keywords Elliptic PDE · Variable coefficients · Boundary-domain integral equation · H-matrices

1 Introduction

A number of profound positive developments in the area of boundary element technique have occurred in the last decade. Despite of that, an efficient numerical treatment of boundary value problems (BVPs) with variable coefficients is often a challenge, because the fundamental solution for the corresponding operator is not available in this case. To remedy this difficulty we follow Hilbert [7] and Levi [8] and replace the fundamental solution with a parametrix (Levi function). This yields a boundary-domain integral or integro-differential formulation of the problem, cf. [9]. Equivalence of these formulations to the original BVP, as well as invertibility of the associated operators can be proved similar to [4,5,10].

In this study, we consider a collocation discretisation of boundary-domain integral and integro-differential equations, BDIDEs, equivalent to the Dirichlet BVP for the partial differential equations of the stationary diffusion (e.g. heat transfer) with scalar variable coefficient. Discretisation of the resulting layer potentials, the volume Newton-type and remainders potential operators produces fully populated matrices. Moreover, in contrast to boundary integral formulations of BVPs with constant coefficients, for the boundary-domain formulations it is necessary to perform volume discretisation even when the right hand side is zero. To avoid prohibitively expensive second order complexity and storage requirements for the fully populated matrices, we implemented the hierarchical matrix compression technique in conjunction with the adaptive cross approximation (ACA) procedure [3]. We comment on the implementation details and report the results of numerical experiments solving BDIDEs for the Dirichlet problem in three-dimensional (3D) domains.

Note that numerical solution of BDIEs for 2D problems is available in [11]. Note also that another way of reducing the matrix size is to introduce localised parametrix, which makes all matrices sparse, cf. [9], and numerical implementation of the latter approach to some 2D BVPs is available in [12,14,15,17–19] and references therein.

2 Boundary domain integral and integro-differential equations

Let us consider the Dirichlet problem for the linear second-order elliptic PDE in a bounded domain $\Omega \subset \mathbb{R}^3$ with a Lipschitz boundary $\Gamma = \partial\Omega$

R. Grzhibovskis (✉) · S. Rjasanow
Saarland University, Saarbrücken, Germany
e-mail: richards@num.uni-sb.de

S. Rjasanow
e-mail: rjasanow@num.uni-sb.de

S. Mikhailov
Brunel University, London, UK
e-mail: Sergey.Mikhailov@brunel.ac.uk

$$Au\,(x) := \sum_{i,j=1}^{3} \frac{\partial}{\partial x_i}\left[a(x)\frac{\partial}{\partial x_j}u(x)\right] = f(x), \quad x \in \Omega,$$
$$\gamma u(x) = \bar{u}(x), \quad x \in \Gamma, \tag{1}$$

where γ is the trace operator, u is the unknown function, while f, $\bar{u}$ and a are prescribed functions and $a(x) \geq a_{min} > 0$, $x \in \Omega$. We will look for a solution of the BVP in the space

$$H^{1,0}(\Omega;\ A) := \{u \in H^1(\Omega) : Au \in L_2(\Omega)\},$$

where $H^1(\Omega)$ is the usual Sobolev space of square integrable functions with square integrable first derivatives.

A parametrix for PDE (1) with variable coefficient, obtained from the fundamental solution for the same equation but with 'frozen' coefficient $a(y)$ is

$$P(x,\ y) = \frac{-1}{4\pi a(y)|x-y|}, \quad x,\ y \in \mathbb{R}^3. \tag{2}$$

It satisfies equation

$$(AP\,(\cdot,\ y))\,(x) = \delta(x-y) + R(x,\ y),$$

where δ is the Dirac delta-distribution, while the remainder, having only a weak singularity at $x = y$, is

$$R(x,\ y) = \frac{1}{4\pi a(y)|x-y|^3}(x-y)\cdot\nabla a(x), \quad x,\ y \in \mathbb{R}^3. \tag{3}$$

Let $Tu(x) = a(x)n(x)\cdot\nabla u(x)$, $x \in \Gamma$ be the co-normal derivative operator.

As shown in [4,5,9,10], for any function u the parametrix-based third Green identity holds in the form

$$u(y) + \int_\Omega R(x,\ y)u(x)\mathrm{d}x + \int_\Gamma P(x,\ y)Tu(x)\mathrm{d}\Gamma(x) - \int_\Gamma u(x)T_x P(x,\ y)\mathrm{d}\Gamma(x) = \int_\Omega P\,(x,\ y)\ f\,(x)\,\mathrm{d}x, \quad y \in \Omega.$$

Then the BVP (1) can be reduced to the following direct united BDIDE at each $y \in \Omega$

$$u(y) + \int_\Gamma P(x,\ y)Tu(x)\mathrm{d}\Gamma(x) + \int_\Omega R(x,\ y)u(x)\mathrm{d}x = \mathcal{F}(y), \tag{4}$$

where

$$\mathcal{F}(y) = \int_\Gamma \bar{u}(x)T_x P(x,\ y)\mathrm{d}\Gamma(x) + \int_\Omega P(x,\ y)f(x)\mathrm{d}x. \tag{5}$$

This equation is integro-differential because of the differential operator T in the left hand side.

On the other hand, similar to [4,9], replacing in equation (4) the co-normal derivative Tu by a new unknown boundary function t and employing the equation in the domain and its trace on the boundary, we arrive at the direct segregated BDIE system with respect to the unknown functions u in Ω and t on Γ,

$$u(y) + \int_\Gamma P(x,\ y)t(x)\mathrm{d}\Gamma(x) + \int_\Omega R(x,\ y)u(x)\mathrm{d}x = \mathcal{F}(y), \quad y \in \Omega, \tag{6}$$

$$\int_\Gamma P(x,\ y)t(x)\mathrm{d}\Gamma(x) + \int_\Omega R(x,\ y)u(x)\mathrm{d}x = -c(y)\bar{u}(y) + \mathcal{F}(y), \quad y \in \Gamma. \tag{7}$$

The same expression (5), where the direct value of the first integral is understood in the Cauchy sense, is to be taken for $\mathcal{F}$ in (7), $c(y) = 1/2$ at the smooth boundary point y, while $c(y) = \alpha(y)/4\pi$ at the corner points, where $\alpha(y)$ is the interior solid angle. BDIE system (6), (7) is called segregated since the function t is considered to be independent of u.

Similar to [4,10] one can show that BDIDE (4) and BDIE system (6), (7) are equivalent to BVP (1) and uniquely solvable, while their left hand side operators are continuous and continuously invertible in appropriate Sobolev spaces. BDIDEs (4) and (6), (7) contain not only the usual surface integrals over the boundary Γ as in the case when the parametrix is a fundamental solution, but also integrals over the entire domain Ω with the unknown function u in the integrand.

3 Discretisation of the segregated and united formulations

We assume, that the domain Ω is given as a union of N_Ω tetrahedral elements, which constitute a conformal 3D mesh with M nodes $\{x_j\}_{j=1}^M$ and N_Γ boundary triangles. In particular, we have

$$\Omega = \bigcup_{i=1}^{N_\Omega} \overline{T}_i, \quad \Gamma = \bigcup_{k=1}^{N_\Gamma} \overline{\tau}_k.$$

We employ the continuous, piecewise linear Ansatz for the unknown function

$$u^h(x) = \sum_{j=1}^{M} u_j \varphi_j(x), \quad x \in \Omega \cup \Gamma,$$

where φ_j is linear on any T_i,

$$\varphi_j(x_k) = \delta_{jk} \quad \text{and } u_j = u^h(x_j).$$

If we denote by M_Ω the number of interior nodes of the mesh, then the number of boundary nodes is

$$M_\Gamma = M - M_\Omega.$$

Assuming that the numbering of nodes starts from the interior ones and taking into account the Dirichlet boundary condition in (1), we can also write u^h as a sum of known and unknown parts

$$u^h(x) = \sum_{j=1}^{M_\Omega} u_j \varphi_j(x) + \sum_{j=M_\Omega+1}^{M} \bar{u}_j \varphi_j(x), \tag{8}$$

where the values $\bar{u}_j = \bar{u}(x_j)$, $j = M_\Omega + 1, \ldots, M$ are known.

The gradient of u is approximated by the piecewise constant function ∇u^h. Thus, the discretized co-normal derivative is constant on each boundary triangle τ_k. Its value reads

$$\begin{aligned} n(x) \cdot \nabla u^h(x) &= n_k \cdot \nabla u^h|_{\tau_k} = \sum_{\{j: x_j \in T_{\tau_k}\}} (n_k \cdot \nabla \varphi_j) u_j \\ &= \sum_{j=1}^{M} \mathbf{T}^{\Delta}_{kj} u_j, \quad x \in \tau_k, \end{aligned} \tag{9}$$

where n_k is the outer normal unit vector to the triangle τ_k and T_{τ_k} denotes the unique volume element, which possesses the triangle τ_k as one of its faces,

$$\mathbf{T}^{\Delta}_{kj} = \begin{cases} n_k \cdot \nabla \varphi_j, & \text{if } x_j \in T_{\tau_k} \\ 0, & \text{if } x_j \notin T_{\tau_k} \end{cases}$$

is the sparse matrix approximating the normal derivative operator on the boundary triangle τ_k.

Substituting (8) and (9) into the *united* BDIDE (4), collocating at the interior nodes x_i, $i = 1, \ldots, M_\Omega$ and shifting the known function values on the boundary Γ in to the right hand side, we arrive at the discrete system of M_Ω equations for M_Ω unknowns u_i, $i = 1, \ldots, M_\Omega$

$$\begin{aligned} &u_i + \sum_{j=1}^{M_\Omega} \left(\sum_{k=1}^{N_\Gamma} \mathbf{V}^a_{ik} \mathbf{T}^{\Delta}_{kj} + \mathbf{R}_{ij} \right) u_j \\ &\quad = \sum_{j=M_\Omega+1}^{M} \left(\mathbf{K}_{ij} - \sum_{k=1}^{N_\Gamma} \mathbf{V}^a_{ik} \mathbf{T}^{\Delta}_{kj} - \mathbf{R}_{ij} \right) \bar{u}_j + \mathbf{f}_i. \end{aligned} \tag{10}$$

The matrices $\mathbf{V}^a \in \mathbb{R}^{M \times N_\Gamma}$, $\mathbf{R} \in \mathbb{R}^{M \times M}$, $\mathbf{K} \in \mathbb{R}^{M \times M_\Gamma}$ in (10) are the discrete versions of the corresponding integral operators, namely

$$\mathbf{V}^a_{ik} = \int_{\tau_k} P(x, x_i)\, a(x)\, \mathrm{d}\Gamma(x), \tag{11}$$

$$\mathbf{K}_{ij} = \int_{\Gamma} T_x P(x, x_i)\, \varphi_j(x)\, \mathrm{d}\Gamma(x), \tag{12}$$

$$\mathbf{R}_{ij} = \int_{\Omega} R(x, x_i)\, \varphi_j(x)\, \mathrm{d}x, \tag{13}$$

and the vector $\mathbf{f} \in \mathbb{R}^M$ can be computed ether as

$$\mathbf{f}_i = \sum_{k=1}^{N_\Omega} \int_{T_k} P(x, x_i)\, f(x)\, \mathrm{d}x, \tag{14}$$

when the function f is given analytically, or as

$$\mathbf{f}_i = \sum_{j=1}^{M} f_j \int_{\Omega} P(x, x_i)\, \varphi_j(x)\, \mathrm{d}x \tag{15}$$

in the case, when the function f is given in the form $f(x) = \sum_{j=1}^{M} f_j \varphi_j(x)$.

In the case of the *segregated* formulation (6), the N_Γ co-normal derivatives $a\mathbf{T}^{\Delta}\mathbf{u}$ are not computed from u^h but are considered as N_Γ auxiliary unknowns $t_k, k = 1, \ldots, N_\Gamma$. This corresponds to the piecewise constant approximation of the Neumann data

$$t(x) = \sum_{k=1}^{N_\Gamma} t_k \psi_k(x), \quad \psi_k(x) = \begin{cases} 1, & \text{when } x \in \tau_k, \\ 0, & \text{otherwise.} \end{cases}$$

Therefore, additional collocation points

$$\tilde{x}_k, \ k = 1, \ldots, N_\Gamma$$

are added in the centers of the boundary triangles τ_k. Thus, the discrete version of the segregated formulation (6) is given by the following system of $M_\Omega + N_\Gamma$ linear algebraic equations for $M_\Omega + N_\Gamma$ unknowns u_j, $j = M_\Gamma + 1, \ldots, M$, and $t_k, k = 1, \ldots, N_\Gamma$,

$$u_i + \sum_{j=1}^{M_\Omega} \mathbf{R}_{ij} u_j + \sum_{k=1}^{N_\Gamma} \mathbf{V}_{ik} t_k = \sum_{j=M_\Omega+1}^{M} \left(\mathbf{K}_{ij} - \mathbf{R}_{ij}\right) \bar{u}_j + \mathbf{f}_i, \quad i = 1, \ldots, M_\Omega, \tag{16}$$

$$\sum_{j=1}^{M_\Omega} \tilde{\mathbf{R}}_{nj} u_j + \sum_{k=1}^{N_\Gamma} \tilde{\mathbf{V}}_{nk} t_k = -\frac{1}{2}\tilde{u}_n + \sum_{j=M_\Omega+1}^{M} \left(\tilde{\mathbf{K}}_{nj} - \tilde{\mathbf{R}}_{nj}\right) \bar{u}_j + \tilde{\mathbf{f}}_n, \quad n = 1, \ldots, N_\Gamma. \tag{17}$$

where the matrix $\mathbf{V}_{ik}$ is given by (11) with a dropped, while elements of the matrix $\tilde{\mathbf{V}}_{nk}$ are given by the same formula (11) (with a dropped) and $\tilde{\mathbf{R}}_{nj}, \tilde{\mathbf{K}}_{nj}, \tilde{\mathbf{f}}_n$ by (12)–(15) with x_j replaced by $\tilde{x}_k$, and $\tilde{u}_n = \bar{u}(\tilde{x}_n)$.

When the united formulation is employed, all collocation nodes lie inside the domain. Therefore, expressions under the surface integrals are smooth. Singularities in the domain integrals are weak and can be handled by means of the Duffy transform. In the case of segregated formulation, values of the weakly singular integrals for entries of $\tilde{\mathbf{V}}$ and Cauchy integrals for entries of $\tilde{\mathbf{K}}$ can be obtained by means of a combination of Gauss integration and analytical formulae found in [13, Chap. C2], see Appendix for more details.

Because of the non-local nature of the parametrix (2) and the remainder (3), the matrices $\mathbf{V}$, $\tilde{\mathbf{V}}$, $\mathbf{K}$, $\tilde{\mathbf{K}}$, $\mathbf{R}$ and $\tilde{\mathbf{R}}$ are fully populated. It is, however, easy to check, that the integration kernels in (11)–(15) are asymptotically smooth [13]. Therefore, after an appropriate reorderings of rows and columns (clustering) the matrices can be efficiently approximated by block-wise low rank matrices by means of the H-matrix/ACA technique [3,13]. This approximation leads to reduction of computational complexity and storage requirements from quadratic to almost linear in terms of M.

4 Compression of matrices by means of the H-Matrix/ACA technique

In this section, we briefly describe the construction of a block-wise low-rank approximant of a matrix

$$\mathbf{\Phi} \in \mathbb{R}^{M\times N}, \quad \mathbf{\Phi}_{ij} = \int_{F} G\left(x,\, x_i\right) \tilde{\psi}_j\left(x\right) \mathrm{d}F\left(x\right),$$

where N is N_Γ, M or M_Γ, and the kernel function G is a product of the parametrix (2) or its derivatives with a smooth function (coefficient a or its derivatives). The integration domain F is either the domain Ω or its boundary Γ. The functions $\tilde{\psi}_j$ are either piecewise linear or piecewise constant basis functions (φ_j or ψ_j respectively). We consider two subsets of $\mathbb{R}^3$,

$$\bigcup_{i=1}^{M} \{x_i\} \quad \text{and} \quad \overline{\Omega} = \bigcup_{j=1}^{N_\Omega} \mathrm{supp}\tilde{\psi}_j.$$

4.1 Low-rank approximation

Suppose that we have found two sets of indices $I \subseteq \{i\}_{i=1}^{M}$ and $J \subseteq \{j\}_{j=1}^{N}$ such that the corresponding subsets

$$\eta = \bigcup_{i\in I} \{x_i\} \quad \text{and } \nu = \bigcup_{j\in J} \mathrm{supp}\tilde{\psi}_j$$

are well separated; that is,

$$\max\left(\mathrm{diam}\,\eta,\ \mathrm{diam}\,\nu\right) \le \theta \mathrm{dist}\left(\eta,\ \nu\right), \tag{18}$$

for some $\theta \in (0,\ 1)$. The diameter of a set is the maximal distance between any pair of points in it. The distance between two sets of points is defined as

$$\mathrm{dist}\left(\eta,\ \nu\right) = \min_{x\in\eta,\ y\in\nu} |x - y|. \tag{19}$$

The idea of the matrix compression is based on the observation, that the corresponding sub-block

$$\left\{\mathbf{\Phi}_{ij},\quad i \in I,\quad j \in J\right\}$$

of the matrix $\mathbf{\Phi}$ has a low-rank approximant provided that the partial derivatives of the kernel function G decay sufficiently fast [1,2]. More precisely, G must be asymptotically smooth, i.e. one must be able to find positive constants C_1 and C_2 and an integer $\alpha_0 \ge 0$ such that for all multi-indices α with $|\alpha| \ge \alpha_0$ and any $R = |x - y| > 0$ it must hold

$$\left|\partial_y^\alpha G\left(x,\ y\right)\right| \le C_1 |\alpha|! C_2^{|\alpha|} R^{-|\alpha|} \sup_{|y-z|<R} |G\left(x,\ z\right)|. \tag{20}$$

Moreover, the rank of the approximant depends only on the separation θ and the desired accuracy of the approximation, but not on the number of entries in clusters I and J. It is easy to check, that the integration kernels in (12)–(15) satisfy (20). Several methods of finding the approximant are available. Although the truncated singular value decomposition produces the approximant with the smallest rank, this procedure is too computationally expensive. An inexpensive alternative uses the interpolation of G as in panel clustering [6], or the algebraic approach as in the ACA algorithm [1–3]. The idea of ACA method consists in finding the approximant as a sum of certain tensor products. The first term in this sum can be taken to be the result of multiplying the first column with the first row of $\mathbf{\Phi}$. The subsequent terms are the products of the m-th column with the k-th row of the difference between $\mathbf{\Phi}$ and already accumulated approximant. The essence of the procedure is in the adaptive choice of the pivot indices m and k. We refer to [3] or [13] for details and analysis of the method.

4.2 Clustering of the index sets

To partition the matrix $\mathbf{\Phi}$ into admissible blocks we employ a hierarchical clustering method similar to that formulated in [1] for a set of boundary elements in $\mathbb{R}^3$. For a given set of indices $\{i\}_1^M$, we construct a cluster tree $\mathcal{T}_1$ as follows:

(1) Let the set of all indices be the root cluster of the tree.
(2) Compute the mass center, and axes of inertia of the corresponding geometric set.
(3) Split the set into two parts by a plane that passes through the center of mass and is orthogonal to the longest axis of inertia.
(4) Assign the indices of the obtained groups of geometric entities as cluster offsprings.
(5) Recursively apply the subdivision procedure to the offsprings so long as the cluster consists of more than one index.

A cluster tree $\mathcal{T}_2$ is then constructed for the second index set $\{j\}_{j=1}^N$. Having computed $\mathcal{T}_1$ and $\mathcal{T}_2$, we can recursively generate a list of disjoint admissible blocks B_A that, together with the additional sparse part B_S, cover the whole matrix $\mathbf{\Phi}$. This can be accomplished by the following recursive procedure:

(1) Set $\eta = \mathcal{T}_1$, $\nu = \mathcal{T}_2$, $B_A = \emptyset$, and $B_S = \emptyset$.
(2) If η or ν has only one element (no offsprings), add $\eta \times \nu$ to B_S and end the procedure.
(3) If $(\eta,\ \nu)$ satisfy (18), add $\eta \times \nu$ to B_A and end the procedure.
(4) Denote by η_1 and η_2 the offsprings of η, and by ν_1 and ν_2 the offsprings of ν. Proceed to Step 2 with $(\eta,\ \nu)$ being $(\eta_1,\ \nu_1)$, $(\eta_1,\ \nu_2)$, $(\eta_2,\ \nu_1)$, or $(\eta_2,\ \nu_2)$.

On completion, the algorithm produces a list of admissible blocks B_A, satisfying (18), and a list B_S of small blocks. We compute all small blocks directly and approximate each admissible block using the ACA procedure.

4.3 Complexity

The overall computational costs of finding the block-wise low-rank approximation to the matrix $\mathbf{\Phi} \in \mathbb{R}^{M\times N}$ is

$$O\left(\tilde{N}\log\tilde{N}|\log\varepsilon|^4\right),\quad \tilde{N} = \max(M,\ N),$$

where ε is the desired accuracy. Once the approximant has been generated, it occupies $O\left(\tilde{N}\log\tilde{N}|\log\varepsilon|^2\right)$ units of storage and the numerical cost of multiplying it with a vector is of the same order (see [2]).

5 Numerical results

In this section we report the results of numerical experiments in 3D and analyze (a) the accuracy of the proposed numerical scheme, (b) efficiency of solving the linear systems (10) and (16)–(17) by an iterative method (generalised minimal residual [GMRES]), (c) effects of the ACA compression of matrices $\mathbf{V}$, $\mathbf{K}$, and $\mathbf{R}$. The function

$$u_{ex}(x) = \left((x_1-\hat{x}_1)^2 + (x_2-\hat{x}_2)^2\right)^{1/2}$$

solves the BVP (1) provided that

$$a(x) = \left((x_1-\hat{x}_1)^2 + (x_2-\hat{x}_2)^2\right)^{-1/2},$$

$(\hat{x}_1,\ \hat{x}_2,\ \hat{x}_3) \notin \Omega$ for any $\hat{x}_3$; $f = 0$ and $\bar{u}(x) = \gamma u_{ex}(x)$ on Γ. We choose the domain to be the cube

$$\Omega = (-0.5,\ 0.5)^3$$

or the ball

$$\Omega = \{x \in \mathbb{R}^3 : |x| < 0.5\}$$

and fix the parameters $(\hat{x}_1,\ \hat{x}_2) = (3,\ 3)$. To investigate the convergence of the method, a sequence of quasi-uniform volume meshes is employed. In this sequence, the spatial discretisation parameter (average element diameter)

$$h = \left(\mathrm{Vol}\,(\Omega)\,/(N_\Omega)\right)^{1/3}$$

varies between 0.16 for the coarsest mesh and 0.016 for the finest one. The convergence results are summarised in Fig. 1, where the relative L^2 error

$$\varepsilon = \|u^h - u_{ex}\|_{L^2(\Omega)}/\|u_{ex}\|_{L^2(\Omega)}$$

is plotted for numerical experiments with the ball-shaped (circular markers) and the cube-shaped (square markers) domain. We observe the convergence of order two for both domains and both united (filled markers) and segregated

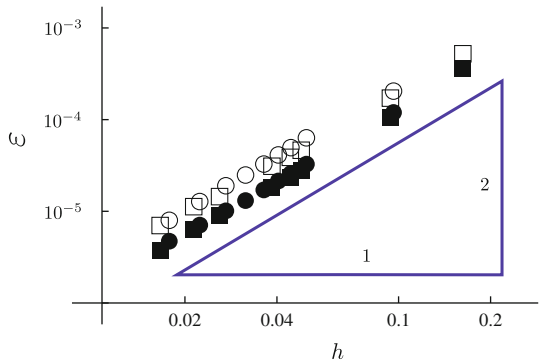

Fig. 1 Convergence of the united (*full markers*) and segregated (*empty markers*) formulations of the BDIDEs for the cases of *ball-shaped* (*round markers*) and *cube-shaped* (*square markers*) domains

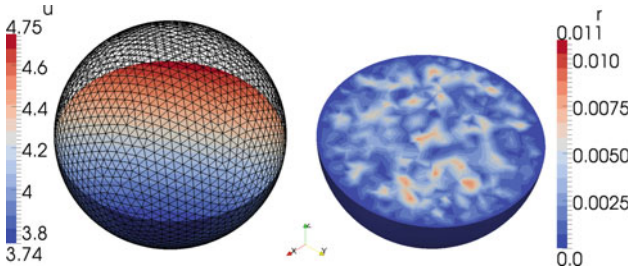

Fig. 2 Distribution of the error inside the ball discretised with $M = 8,967$ nodes

(empty markers) formulations. The distribution of the absolute point-wise error

$$r(x) = |u^h(x) - u_{ex}(x)|$$

inside the ball-shaped domain for the discretisation with $M = 8,967$ nodes is illustrated in Fig. 2. The error appears to have an almost uniform distribution inside the volume with a maximum of about 0.25 %. Approximate solutions to systems (10) and (16)–(17) were obtained by the GMRES iterative procedure. The number of unknowns is M_Ω in the case of the united formulation and $M_\Omega + N_\Gamma$ in the case of the segregated formulation. The dependence of number of GMRES iterations necessary to achieve the residuum of 10^{-9} on the number of unknowns is shown in Fig. 3 (top). In the case of the segregated formulation the Jacobi preconditioning was applied. We see, that for both domains the number of iterations is proportional to the logarithm of the number of the unknowns. The proportionality coefficient, however, is considerably higher in the case of the segregated formulation (empty markers).

The effects of the H-matrix/ACA compression on the matrix R for the ball-shaped domain are shown in Fig. 3 (bottom). We observe, that practical benefits of the compression technique first appear when the number of nodes is greater than 5,000. For these values of M the size of the compressed matrix grows almost linearly.

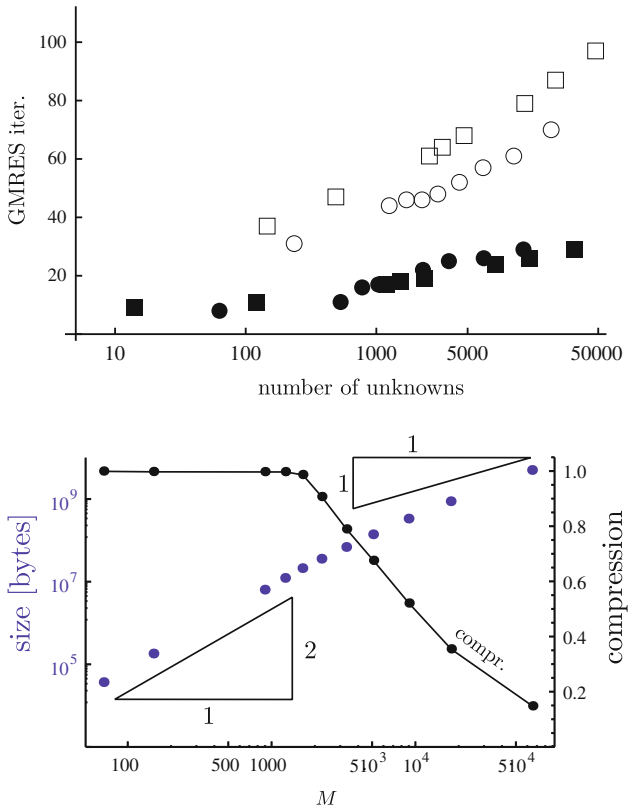

Fig. 3 Performance of the H-matrix/ACA accelerated collocation solver. Dependence of the number of GMRES iterations on the problem size (*top*). The size and the compression ratio of the matrix **R** for the ball-shaped geometry (*bottom*)

The method can be further developed to include the meshless discretisation of the domain and the use of localised parametrix as well as application to more general domains and equations, e.g. of elasticity and elasto-plasticity.

Acknowledgments The partial support from the EPSRC Grant EP/H020497/1: "Mathematical Analysis of Localised Boundary-Domain Integral Equations for Variable-Coefficients Boundary Value Problems" is gratefully acknowledged.

6 Conclusions

The collocation discretisation of BDIDEs for the Dirichlet problem of the stationary diffusion (e.g. heat transfer) partial differential equation with variable coefficient yields a numerical method with second order accuracy for the unknown function. The number of GMRES iterations for the approximate solution of the resulting linear system grows logarithmically as the number of unknowns increases. The H-matrix/ACA compression technique makes it possible to efficiently approximate the fully populated matrices of the integral operators.

Appendix: Matrix entries calculation

We present here in more details the algorithms used for calculation of matrices (11)–(15) in the considered examples. Coefficients for 2D and 3D quadrature rules are taken from [16].

Matrix **R**

We consider the entries of the matrix **R**

$$\mathbf{R}_{jm} = \int\limits_{\operatorname{supp}\varphi_m} R\left(x,\, x_j\right)\varphi_m\left(x\right)\,\mathrm{d}x = \sum_{k=1}^{N_m}\mathbf{R}_{jm}^{k},$$

where

$$\mathbf{R}_{jm}^{k} := \int\limits_{T_{mk}} R\left(x,\, x_j\right)\varphi_m\left(x\right)\,\mathrm{d}x$$

$$= \frac{1}{4\pi a\left(x_j\right)}\int\limits_{T_{mk}} \frac{\left(x-x_j\right)\cdot\nabla a\left(x\right)}{|x-x_j|^3}\varphi_m\left(x\right)\,\mathrm{d}x. \tag{21}$$

Here tetrahedrons T_{mk}, $k = 1,\ldots,N_m$ constitute the support of φ_m (i.e. comprise all tetrahedrons, which have x_m as a node).

Since x_j is a node, we distinguish the following three cases.

(1) Let x_j lie outside of T_{mk}. Then the integrand in (21) in smooth and $\mathbf{R}_{jm}^{k}$ was approximated by the fifth order Gauss quadrature formula with 17 points.

(2) Let x_j be among vertices of T_{mk}, but $x_j \neq x_m$. We denote the vertices of the tetrahedron T_{mk} as $\{x_j,\, x_m,\, x_\alpha,\, x_\beta\}$. Since the integrand in (21) has the weak singularity of the order $1/r$, we used the Duffy transform, introducing the new integration variables u, v, and w through

$$x\left(u,\, v,\, w\right) = x_j + u\mathsf{v}_1 + uv\mathsf{v}_2 + uvw\mathsf{v}_3,$$

where $\mathsf{v}_1 = x_m - x_j$, $\mathsf{v}_2 = x_\alpha - x_m$, $\mathsf{v}_3 = x_\beta - x_\alpha$. In these new variables the integral becomes

$$\mathbf{R}_{jm}^{k} = \frac{3|T_{mk}|}{2\pi a\left(x_j\right)}\int_0^1\int_0^1 \frac{v(1-v)}{|\mathsf{v}_1 + v\mathsf{v}_2 + vw\mathsf{v}_3|^3} \times \int_0^1 u\frac{\partial a}{\partial u}\,\mathrm{d}u\,\mathrm{d}v\,\mathrm{d}w, \tag{22}$$

where $|T_{mk}|$ is the volume of the tetrahedron T_{mk}. Partial integration over u yields

$$\int_0^1 u\frac{\partial a}{\partial u}\,\mathrm{d}u = a\left(x\left(1,\, v,\, w\right)\right) - \int_0^1 a\left(x\left(u,\, v,\, w\right)\right)\,\mathrm{d}u,$$

which makes the computation of integrand in (22) free from derivatives of the coefficient function a. The resulting expression becomes

$$\mathbf{R}_{jm}^{k} = \frac{6|T_{mk}|}{4\pi a\left(x_j\right)} \times \left[\int_0^1\int_0^1 \frac{v(1-v)a\left(x\left(1,\, v,\, w\right)\right)}{|\mathsf{v}_1 + v\mathsf{v}_2 + vw\mathsf{v}_3|^3}\,\mathrm{d}v\,\mathrm{d}w - \int_0^1\int_0^1\int_0^1 \frac{v(1-v)a\left(x\left(u,\, v,\, w\right)\right)}{|\mathsf{v}_1 + v\mathsf{v}_2 + vw\mathsf{v}_3|^3}\,\mathrm{d}u\,\mathrm{d}v\,\mathrm{d}w\right]$$

which is approximated by a product Gauss–Kronrod quadrature formula, where the approximate integration of order 31 (21 points) is used for each 1D integral.

(3) Let $x_j = x_m$. We denote the vertices of the tetrahedron T_{mk} are $\{x_j,\, x_\alpha,\, x_\beta,\, x_\gamma\}$. Since the integrand in (21) has for this case the weak singularity of the order $1/r^2$, we used the Duffy transform, introducing the new integration variables through

$$x\left(u,\, v,\, w\right) = x_m + u\mathsf{v}_1 + uv\mathsf{v}_2 + uvw\mathsf{v}_3,$$

where $\mathsf{v}_1 = x_m - x_\alpha$, $\mathsf{v}_2 = x_\beta - x_\alpha$, $\mathsf{v}_3 = x_\gamma - x_\beta$. In these new variables the integral becomes

$$\mathbf{R}_{jm}^{k} = \frac{3|T_{mk}|}{2\pi a\left(x_j\right)}\int_0^1\int_0^1 \frac{v}{|\mathsf{v}_1 + v\mathsf{v}_2 + vw\mathsf{v}_3|^3} \times \int_0^1 (1-u)\frac{\partial a}{\partial u}\,\mathrm{d}u\,\mathrm{d}v\,\mathrm{d}w. \tag{23}$$

Partial integration over u yields

$$\int_0^1 (1-u)\frac{\partial a}{\partial u}\,\mathrm{d}u = \int_0^1 a\left(x\left(u,\, v,\, w\right)\right)\,\mathrm{d}u - a\left(x_m\right),$$

which makes the computation of integrand in (23) free from derivatives of the coefficient function a. The resulting expression becomes

$$\mathbf{R}_{jm}^{k} = \frac{3|T_{mk}|}{2\pi a\left(x_j\right)} \times \left[\int_0^1\int_0^1\int_0^1 \frac{v(1-v)a\left(x\left(u,\, v,\, w\right)\right)}{|\mathsf{v}_1 + v\mathsf{v}_2 + vw\mathsf{v}_3|^3}\,\mathrm{d}u\,\mathrm{d}v\,\mathrm{d}w - a\left(x_m\right)\int_0^1\int_0^1 \frac{v}{|\mathsf{v}_1 + v\mathsf{v}_2 + vw\mathsf{v}_3|^3}\,\mathrm{d}v\,\mathrm{d}w\right],$$

which is approximated by a product Gauss–Kronrod quadrature formula, where the approximate integration of order 31 (21 points) is used for each 1D integral.

Matrix $\mathbf{V}^a$

We consider the entries of the matrix $\mathbf{V}^a$

$$\mathbf{V}^a_{jk} = \int\limits_{\tau_k} P\left(x,\, x_j\right) a\left(x\right) \mathrm{d}\Gamma\left(x\right) = -\frac{1}{4\pi a\left(x_j\right)} \int\limits_{\tau_k} \frac{a\left(x\right)}{|x - x_j|} \mathrm{d}\Gamma\left(x\right),$$

where τ_k is a boundary triangle. We distinguish the following two cases.

(1) Let x_j be outside of τ_k. We decompose the integral into two parts,

$$\mathbf{V}^a_{jk} = -\frac{1}{4\pi a\left(x_j\right)} \left[a\left(x_j\right) \int\limits_{\tau_k} \frac{1}{|x - x_j|} \mathrm{d}\Gamma\left(x\right) + \int\limits_{\tau_k} \frac{a\left(x\right) - a\left(x_j\right)}{|x - x_j|} \mathrm{d}\Gamma\left(x\right) \right]. \tag{24}$$

The first integral is computed by an exact analytical formula, see [13, Chap. C2.2], while the second one is approximated by the 13th order Gauss quadrature formula with 37 points.

(2) Let x_j be among the vertices of τ_k. We denote the vertices of the triangle τ_k as $\left\{x_j,\, x_\alpha,\, x_\beta\right\}$ and use the Duffy transform introducing the new integration variables u and v through

$$x\left(u,\, v\right) = x_j + u\mathsf{v}_1 + uv\mathsf{v}_2,$$

where $\mathsf{v}_1 = x_\alpha - x_j$, $\mathsf{v}_2 = x_\beta - x_\alpha$. Then the integral becomes

$$\mathbf{V}^a_{jk} = -\frac{2|\tau_k|}{4\pi a\left(x_j\right)} \int\limits_0^1 \int\limits_0^1 \frac{a\left(x\left(u,\, v\right)\right)}{|\mathsf{v}_1 + v\mathsf{v}_2|} \mathrm{d}u\, \mathrm{d}v,$$

where $|\tau_k|$ is the area of the triangle. The integral is approximated by a product Gauss–Kronrod quadrature formula, where the approximate integration of order 31 (21 points) is used for each 1D integral.

Matrix $\mathbf{K}$

We consider the entries of the matrix $\mathbf{K}$

$$\mathbf{K}_{jm} = \int\limits_{\Gamma} T_x P\left(x,\, x_j\right) \varphi_m\left(x\right) \mathrm{d}\Gamma\left(x\right) = \sum_{k=1}^{N_{\Gamma m}} \mathbf{K}^k_{jm},$$

where

$$\mathbf{K}^k_{jm} := -\frac{1}{4\pi a\left(x_j\right)} \times \int\limits_{\tau_{km}} \frac{\left(x - x_j\right) \cdot n_{\tau_{km}}}{|x - x_j|^3} a\left(x\right) \varphi_m\left(x\right) \mathrm{d}\Gamma\left(x\right).$$

Here the boundary triangles τ_{km}, $k = 1, \ldots, N_{\Gamma m}$ have the node x_m as a vertex. We distinguish the following two cases.

(1) Let x_j be outside of τ_{km}. We decompose the integral into two parts

$$\mathbf{K}^k_{jm} = \frac{1}{4\pi a\left(x_j\right)} \times \left[a\left(x_j\right) \int\limits_{\tau_{km}} \frac{\left(x - x_j\right) \cdot n_{\tau_{km}}}{|x - x_j|^3} \varphi_m\left(x\right) \mathrm{d}\Gamma\left(x\right) + \int\limits_{\tau_{km}} \frac{\left(x - x_j\right) \cdot n_{\tau_{km}}}{|x - x_j|^3} \left(a\left(x\right) - a\left(x_j\right)\right) \varphi_m\left(x\right) \mathrm{d}\Gamma\left(x\right) \right].$$

The first integral is computed by an exact analytical formula, see [13, Chap. C2.2], while the second one is approximated by the 13th order Gauss quadrature formula with 37 points.

(2) Let x_j be among vertices vertices of τ_{km}. In this case the vector $\left(x_j - x\right)$ is orthogonal to $n_{\tau_{km}}$ and, thus, $\mathbf{K}^k_{jm} = 0$.

References

1. Bebendorf M (2000) Approximation of boundary element matrices. Numer Math 86(4):565–589
2. Bebendorf M, Grzhibovskis R (2006) Accelerating Galerkin BEM for linear elasticity using adaptive cross approximation. Math Methods Appl Sci 29(14):1721–1747
3. Bebendorf M, Rjasanow S (2003) Adaptive low-rank approximation of collocation matrices. Computing 70:1–24
4. Chkadua O, Mikhailov SE, Natroshvili D (2009) Analysis of direct boundary-domain integral equations for a mixed BVP with variable coefficient, I: equivalence and invertibility. J Integr Equ Appl 21(4):499–543

5. Chkadua O, Mikhailov SE, Natroshvili D (2011) Analysis of segregated boundary-domain integral equations for variable-coefficient problems with cracks. Numer Methods Partial Differ Equ 27: 121–140
6. Hackbusch W, Nowak ZP (1989) On the fast matrix multiplication in the boundary element method by panel clustering. Numer Math 54(4):463–491
7. Hilbert D (1912) Grundzüge einer allgemeinen Theorie der linearen Integralgleichungen. B. G. Teubner
8. Levi EE (1910) I problemi dei valori al contorno per le equazioni lineari totalmente ellittiche alle derivate parziali. Mem Soc Ital delle Sci 16(3):3–113
9. Mikhailov SE (2002) Localized boundary-domain integral formulations for problems with variable coefficients. Eng Anal Bound Elem 26(8):681–690
10. Mikhailov SE (2006) Analysis of united boundary-domain integro-differential and integral equations for a mixed BVP with variable coefficient. Math Methods Appl Sci 29(6):715–739
11. Mikhailov SE, Mohamed NA (2012) Numerical solution and spectrum of boundary-domain integral equation for the Neumann BVP with variable coefficient. Int J Comput Math 1–17. doi:10.1080/00207160.2012.679733
12. Mikhailov SE, Nakhova IS (2005) Mesh-based numerical implementation of the localized boundary-domain integral-equation method to a variable-coefficient Neumann problem. J Eng Math 51(3):251–259
13. Rjasanow S, Steinbach O (2007) The fast solution of boundary integral equations. Springer, Berlin
14. Sladek J, Sladek V, Atluri SN (2000) Local boundary integral equation (LBIE) method for solving problems of elasticity with nonhomogeneous material properties. Comput Mech 24:456–462
15. Sladek J, Sladek V, Zhang Ch (2005) Local integro-differential equations with domain elements for the numerical solution of partial differential equations with variable coefficients. J Eng Math 51:261–282
16. Stroud A (1971) Approximate calculation of multiple integrals. Prentice-Hall Inc., Englewood Cliffs
17. Taigbenu AE (1999) The Green element method. Kluwer, Dordrecht
18. Zhu T, Zhang J-D, Atluri SN (1998) A local boundary integral equation (LBIE) method in computational mechanics, and a meshless discretization approach. Comput Mech 21:223–235
19. Zhu T, Zhang J-D, Atluri SN (1999) A meshless numerical method based on the local boundary integral equation (LBIE) to solve linear and non-linear boundary value problems. Eng Anal Bound Elem 23:375–389